Journal of Engg. Research **Vol. 4 No. (3) September 2016** pp. 144-162

تحليل الطاقة و exergy لنظام تكييف سقفي يعمل مع مبردات مختلفة

أ. أوزبك

جامعة كوكوروفا، كلية الهندسة بسيهان، قسم الهندسة الميكانيكية، أضنة، تركيا

الخلاصة

في هذه الدراسة، يتم تطبيق تحليل الطاقة وال exergy إلى نظام تكييف الهواء الثقفي الذي يعمل مع مختلف المبردات. أولا، يتم تحديد قدرات تحميل التبريد في الساعة لمبنى في شهور أبريل، مايو، يونيو، يوليو، أغسطس وسبتمبر. ثم يتم تحديد حمولة التبريد باستخدام برنامج تحليل الساعة (HAP). ثانيا، يتم تحديد معامل الأداء، وكفاءة ال exergy وقيم تدمير ال exergy للنظام برمته وكل مكون من مكوناته. وتشير النتائج إلى أن تدمير ال exergy في الأنبوب الضاغط والمكثف والانبوب الشعري ينخفض عند استخدام نظام التبريد R600a في نظام تكييف الهواء الثقفي بدلا من المبردات R404A، ولكن ذلك لا يغير من قيمة الدمار exergy في المبخر بقيمة كبيرة. عند تغيير التبريد من نظام R404A إلى نظام R600a، يتم حساب استهلاك الطاقة ونسبة الدمار exergy ونجد أن الانخفاض في نظام تكييف الهواء يكون بنسبة 13.0% و 20.2% على التوالي، ولكن قيمة كفاءة exergy تزداد بنسبة 13.9%.

Energy and exergy analysis of a ceiling-type air conditioning system operating with different refrigerants

A. Ozbek*

Department of Mechanical Engineering, Ceyhan Engineering Faculty, Cukurova University, 01950, Adana, Turkey

* *Corresponding author: arozbek@cu.edu.tr*

ABSTRACT

In this study, an energy and exergy analysis is applied to a ceiling-type air conditioning (CTAC) system operating with various refrigerants. Firstly, the hourly cooling load capacities of a sample building are determined for the months of April, May, June, July, August and September. The cooling load capacity is determined using the hourly analysis program (HAP). Secondly, the coefficient of performance (COP), exergy efficiency and exergy destruction values of the whole system, and each of its components, are determined. Results indicate that the exergy destruction in the compressor, condenser and capillary tube decreases, when refrigerant R600a is used in the CTAC system instead of refrigerant R404A, but the value of exergy destruction in the evaporator does not substantially change. When the refrigerant is changed from R404A to R600a, it is calculated that the power consumption and exergy destruction ratio of the air conditioning system decrease by 13.0 % and 20.2 %, respectively, but the exergy efficiency value is increased by 13.9 %.

Keywords: Ceiling-type air conditioning system; exergy analysis; exergy destruction; exergy efficiency; exergy rate.

NOMENCLATURE

COP	coefficient of performance	*Subscripts*	
c_p	specific heat [$kJkg^{-1}K^{-1}$]	0	reference (dead) state
$\dot{Ex}$	exergy rate [kW]	act	actual
I	solar radiation [Wm^{-2}]	a	air
$\dot{m}$	mass flow rate [kgs^{-1}]	app	appliance
$\dot{Q}$	heat transfer rate [kW]	atm	atmospheric
T	temperature [^{o}C or K]	buil	building
$\dot{W}$	work [kW]	c	condensation

Greek Letter

η	exergy efficiency
ψ	flow (specific) exergy [$kJkg^{-1}$]

cap	capillary tube
comp	compressor
cond	condenser
dest	destruction
e	evaporation
elec	electric
evap	evaporator
in	incoming
ind	indoor
inf	infiltration
lat	latent
lig	lighting
occ	occupant
out	outgoing
op	opaque
sen	sensible
R	refrigeration system
ref	refrigerant
rev	reversible
tot	total
win	window

INTRODUCTION

In recent years, residential and ceiling-type air conditioning (CTAC) systems have been widely used in household applications all over the world because of their low noise generation, ease of installation and high efficiency values. This type of air conditioning system operates with different refrigerants such as CFCs, HCFCs and HCs. The depletion of the ozone layer and global warming are an important part of the major environmental problems that the world is facing today. The traditional refrigerant fluids, i.e. CFCs and HCFCs, are banned by the Montreal Protocol (1987) because of their contribution to the disruption of the stratospheric ozone layer. The Kyoto Protocol (1997) listed hydrofluorocarbons as having a large global warming potential (GWPs) (Aprea *et al.*, 2013). Consequently, in the long term, refrigerants with low greenhouse warming potential (GWP) are to be used in refrigeration and air conditioning applications. At the same time, the performance of refrigeration and air conditioning equipment has to be improved to reduce the indirect greenhouse warming caused by the use of electricity generated mainly by the combustion of fossil fuels (Bolaji, 2012).

There are many studies about the energy and exergy analysis of air conditioning systems using different refrigerants. Joudi & Al-Amir (2014) experimentally studied a residential type air conditioning system using R22 and alternative refrigerants. They defined system performance parameters such as optimum refrigerant charge, coefficient of performance, cooling capacity, power consumption and pressure ratio. They tested all refrigerants operating in cooling mode under high atmospheric air temperatures, of up to 55 ^{o}C, to discover their suitability. Sun *et al.* (2013) examined the exergy analysis of multi-functional heat pump systems under different operating modes and identified the effects of component structure, working conditions and operating mode on the system operating performance. Bayrakci & Ozgur (2009) explained that exergy destruction for different refrigerants is higher for higher condensing temperatures. When there are greater temperature differences between the atmospheric air and the refrigerant, the exergy destruction will be greater. Kalaiselvam & Saravanan (2009) investigated exergy analysis of a scroll compressor working with R22, R407C and R417A as refrigerants in an HVAC system. They showed that exergy efficiency decreases with an increase in condensing temperature for all refrigerant types. Moreover, they explained that the system should be operated at a condensing temperature between 35 ^{o}C to 40 ^{o}C to obtain good second law efficiency. Arora & Kaushik (2008) presented a detailed exergy analysis of an actual vapor compression refrigeration (VCR) cycle. They developed a model to compute COP, exergy destruction, exergetic efficiency and efficiency defects for R502, R404A and R507A refrigerants, and repeated their experiment for different ranges of evaporator and condenser temperatures. Kabul *et al.* (2008) accomplished first and second law analyses of a vapor compression refrigeration cycle using R600a. They showed that the COP value of the system and its exergy efficiency values decreased, but the total irreversibility rate increased with increasing condenser temperature. Yan *et al.* (2015) improved a modified vapor compression refrigeration cycle operating with a mixture of refrigerants (R290/R600a) for domestic refrigerator-freezers. They introduced a phase separator into the system to enhance the overall system performance and completed a theoretical energy and exergy analysis of the system performance using a mathematical model they developed; they then compared that to the conventional vapor compression refrigeration cycle operating with refrigerant R600a and with the refrigerant mixture, respectively. Padilla *et al.* (2010) carried out an exergy analysis for a domestic refrigerator system with a single evaporator over different evaporation and condensation temperatures ranges using R12 and R413A refrigerants. An experimental performance study of a split air conditioning system using ozone-friendly alternative refrigerants is presented by Bolaji (2012). He designed a split air conditioner with R22 as the working fluid and then retrofitted it with R410A and R417A refrigerants, respectively. Menlik *et al.* (2014) performed second law analysis of an environmentally friendly R290/R600/R600a mixture, at a rate of 45/46/9 % by mass fraction, on a heat pump system as a substitute for R134a. They estimated the value of coefficient of performance, exergy efficiency, exergy destruction, relative irreversibility and improvement potential related to their experimental system. Aprea *et al.* (2013) experimentally compared a commercial R134a refrigeration plant and a CO_2 (R744) system. Exergetic analysis was carried out on the overall experimental device and on the components of the device.

As can be seen from these previous studies, there hasn't been enough study of an air conditioning system working with many refrigerants at the same time. In this study, the energy and exergy analyses of a CTAC system with many different refrigerants has been carried out. In this case, typical refrigerants R404A, R410A, R507, R502, R407C, R22, R290, R134a, R500 and R600a were selected for use in the air conditioning system. A sample building located in Adana province was chosen and the cooling load of the building was then calculated. An inverter-type split air conditioning system operating with these refrigerants was used in order to satisfy the cooling load for the building. The effects of different refrigerants on the refrigeration system and each of the system components were also examined in detail. The study also investigates, which refrigerant is a good alternative for a CTAC system by considering the GWP values.

MATERIAL AND METHODS

Analysis of the vapor compression refrigeration cycle

Mass, energy and exergy balances are applied in order to estimate the heat transfer values from the condenser and evaporator, the COP value, exergy destruction and exergy efficiency values of the refrigeration system and the system components. The general mass balance equation with multiple inlets and outlets can be expressed in rate form as presented by Dincer & Rosen (2007):

$$\sum \dot{m}_{in} = \sum \dot{m}_{out} \tag{1}$$

where $\dot{m}_{in}$ and $\dot{m}_{out}$ are the total rates of mass flow rate into and out of the control volume. The energy balance is expressed in the rate form as:

$$\dot{E}_{in} = \dot{E}_{out} \tag{2}$$

where the subscripts "*in*" and "*out*" indicate the rate of net incoming and outgoing energy transfers by heat, work and mass respectively. Note that energy can be transferred by heat, work and mass only. The energy balance for a general steady-flow system can also be written more explicitly as follows (Cengel & Boles 2004):

$$\dot{Q}_{in} + \dot{W}_{in} + \sum_{in} \dot{m}\left(h + \frac{V^2}{2} + gz\right) = \dot{Q}_{out} + \dot{W}_{out} + \sum_{out} \dot{m}\left(h + \frac{V^2}{2} + gz\right) \quad (3)$$

where h is the enthalpy value per unit mass.

The general exergy balance is expressed in the rate form as:

$$\dot{E}x_{in} - \dot{E}x_{out} = \dot{E}x_{dest} \quad (4)$$

where $\dot{E}x_{in} - \dot{E}x_{out}$ stands for the rate of net exergy transfer by heat, work and mass. $\dot{E}x_{dest}$ also stands for the rate of net exergy destruction. The general exergy balance can also be written as:

$$\dot{E}x_{heat} - \dot{E}x_{work} + \dot{E}x_{mass,in} - \dot{E}x_{mass,out} = \dot{E}x_{dest} \quad (5)$$

The rate of formation of the general exergy balance can also be written as (Hurdogan *et al.*, 2011):

$$\sum\left(1 - \frac{T_o}{T_k}\right)\dot{Q}_k - \dot{W} + \sum \dot{m}_{in}\psi_{in} - \sum \dot{m}_{out}\psi_{out} = \dot{E}x_{dest} \quad (6)$$

where $\dot{W}$ is the work rate, ψ is the flow (specific) exergy and the subscript zero indicates properties at the reference (dead) state of P_0 and T_0. Reference temperature and pressure values used in the calculations are taken to be the temperature of the environment at the time of maximum cooling load, and the pressure calculated according to the height of the province above sea level. The specific flow exergy of refrigerant, or air, is calculated as:

$$\psi_{ref,a} = (h - h_0) - T_0(s - s_0) \quad (7)$$

The exergy rate is determined to be:

$$\dot{E}x = \dot{m}\psi \quad (8)$$

Exergy efficiency of various steady-flow devices can be described from its general definition:

$$\eta = \frac{\dot{E}x_{out}}{\dot{E}x_{in}} \quad (9)$$

The energy-based efficiency measure of the refrigeration unit is explained in terms of electrical input as follows:

$$COP_R = \frac{\dot{Q}_{evap}}{\dot{W}_{comp,act}} \quad (10)$$

where $\dot{Q}_{evap}$ is the heat transfer rate absorbed by the evaporator, $W_{comp,act}$ is the electrical power input to the compressor motor.

Reversible power is the minimum power that is needed to be supplied to the compressor and is defined as:

$$\dot{W}_{comp,rev} = \dot{W}_{comp,act} - \dot{E}x_{dest} = \dot{E}x_{out,comp} - \dot{E}x_{in,comp} \tag{11}$$

Energy and exergy analysis for the system components

The schematic layout of the CTAC system and its components (compressor, condenser, capillary tube and evaporator) are shown in Figure 1. Condensation temperature is taken to be 15 °C which is warmer than the atmospheric temperature ($T_c=T_{atm}+15$ °C). Also, the evaporation temperature is taken to be 15 °C, which is colder than the indoor temperature ($T_e=T_{ind}-15$ °C). The temperature of the refrigerant at state 1 (T_1), shown in Figure 1, is assumed to be 10 °C higher than the evaporation temperature ($T_1=T_e+10$ °C). The temperature of the refrigerant at state 3 (T_3) is assumed to be 10 °C below the condensation temperature of the refrigerant ($T_3=T_c-10$ °C). Thus, the refrigerant leaves the condenser as a compressed liquid and enters the compressor as a superheated vapor.

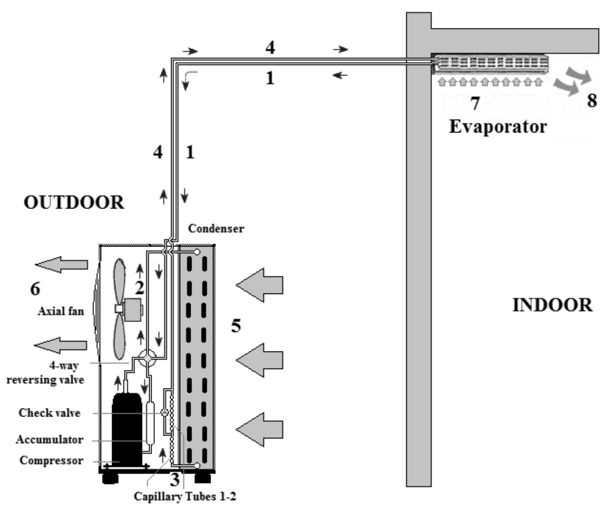

Fig. 1. Schematic diagram of the CTAC system components

The following assumptions have been made during the energy and exergy analyses:

a) All processes are steady-state and steady-flow, with negligible potential and kinetic energy effects.

b) Atmospheric air behaves like an ideal gas with a constant specific heat.

c) The heat transfer and refrigerant pressure drops in tubing and related components are negligible.

d) Heat losses and gains from the condenser and evaporator are ignored.

Mass, energy balance, exergy destruction and exergy efficiency for each of the system components can be represented as follows (Hurdogan *et al.*, 2011):

Compressor:

$$\dot{m}_1 = \dot{m}_2 = \dot{m}_{ref} \tag{12}$$

$$\dot{W}_{comp,act} = \dot{m}_{ref}(h_2 - h_1) \tag{13}$$

$$\dot{E}x_{dest,comp} = \dot{m}_{ref}(\psi_1 - \psi_2) + \dot{W}_{comp,act} \tag{14}$$

$$\eta_{comp} = \frac{\dot{E}x_2 - \dot{E}x_1}{\dot{W}_{comp,act}} \tag{15}$$

Condenser:

$$\dot{m}_2 = \dot{m}_3 = \dot{m}_{ref} \quad ; \qquad \dot{m}_5 = \dot{m}_6 = \dot{m}_{air} \tag{16}$$

$$\dot{Q}_{cond} = \dot{m}_{ref}(h_2 - h_3) = \dot{m}_{air}c_{p,air}(T_6 - T_5) \tag{17}$$

$$\dot{E}x_{dest,cond} = \dot{m}_{ref}(\psi_2 - \psi_3) + \dot{m}_{air}(\psi_5 - \psi_6) \tag{18}$$

$$\eta_{cond} = \frac{\dot{m}_{air}(\psi_6 - \psi_5)}{\dot{m}_{ref}(\psi_2 - \psi_3)} \tag{19}$$

Capillary Tube:

$$\dot{m}_3 = \dot{m}_4 = \dot{m}_{ref} \tag{20}$$

$$h_3 = h_4 \tag{21}$$

$$\dot{E}x_{cap} = \dot{m}_{ref}(\psi_3 - \psi_4) \tag{22}$$

$$\eta_{cap} = \frac{\psi_4}{\psi_3} \tag{23}$$

Evaporator:

$$\dot{m}_1 = \dot{m}_4 = \dot{m}_{ref} \quad ; \qquad \dot{m}_7 = \dot{m}_8 = \dot{m}_{air} \tag{24}$$

$$\dot{Q}_{evap} = \dot{m}_{ref}(h_1 - h_4) = \dot{m}_{air} c_{p,air}(T_7 - T_8) \tag{25}$$

$$\dot{E}x_{dest,evap} = \dot{m}_{ref}(\psi_4 - \psi_1) + \dot{m}_{air}(\psi_7 - \psi_8) \tag{26}$$

$$\eta_{evap} = \frac{\dot{m}_{ref}\psi_1 + \dot{m}_{air}\psi_8}{\dot{m}_{ref}\psi_4 + \dot{m}_{air}\psi_7} \tag{27}$$

Overall exergy efficiency of the refrigeration system:

$$\eta_R = \frac{\dot{E}x_{in,evap} - \dot{E}x_{out,evap}}{\dot{W}_{comp,act}} \tag{28}$$

Total exergy destruction of the refrigeration system:

$$\dot{E}x_{dest,R} = \dot{E}x_{dest,comp} + \dot{E}x_{dest,cond} + \dot{E}x_{dest,cap} + \dot{E}x_{dest,evap} \tag{29}$$

Cooling load analysis

The cooling load design allows for all the loads experienced by a sample building under assumed conditions. The total cooling load consists of heat transferred to the building envelope (walls, doors, roof, floor, windows, etc.) and heat generated by equipment, occupants and lights (Solmaz *et al.*, 2014). The heat transfer rate through opaque surfaces such as the wall, door, floor, roof etc., is given by:

$$\dot{Q}_{op} = U_{op}.A_{op}.CLTD \tag{30}$$

where U_{op} is the overall heat transfer coefficient and A_{op} is the heat transfer area of the surface on the side of the building. *CLTD* is the cooling load temperature difference. The heat transfer through glass is given by:

$$\dot{Q}_{win} = A_{win}[U_{win}(T_o - T_i) + SHGF_{max}.SC] \tag{31}$$

where A_{win} and U_{win} are the surface area and the heat transfer coefficient of the window, respectively. T_o and T_i are the outdoor and indoor air temperatures, $SHGF_{max}$ and SC are the maximum solar heat gain factor and shading coefficient, respectively.

In addition to these external loads, there are the inertial loads because of equipment, appliances, lighting and occupants. Therefore, the sensible cooling load, $\dot{Q}_{sen,buil}$, the latent cooling load, $\dot{Q}_{lat,buil}$ and total cooling load, $\dot{Q}_{tot,buil}$ for the building are obtained by:

$$\dot{Q}_{sen,buil} = \dot{Q}_{op} + \dot{Q}_{win} + \dot{Q}_{sen,inf} + \dot{Q}_{sen,occ} + \dot{Q}_{lig} + \dot{Q}_{sen,app} \quad (32)$$

$$\dot{Q}_{lat,buil} = \dot{Q}_{lat,inf} + \dot{Q}_{lat,occ} + \dot{Q}_{lat,app} \quad (33)$$

$$\dot{Q}_{tot,buil} = \dot{Q}_{sen,buil} + \dot{Q}_{lat,buil} \quad (34)$$

RESULTS AND DISCUSSIONS

Determination of hourly variation of cooling load capacity of the building

Because the maximum cooling load in summer months in Adana occurs in a south-westerly direction, a room facing the south-west of the building was selected as the building sample. Figure 2 presents a schematic view of a sample building with 37 m^2 of floor area located in the Adana province of Turkey. The wall thickness of the building, including brick, insulation and other layers, is taken to be 0.2 m. The hourly cooling load capacity of the building located in the south-westerly direction is calculated by considering double glazed windows in both south and west directions. The northern and eastern sides are adjacent to the inner sides of the building. Double glazed window panes consist of inner glass with a thickness of 6 mm and a reflective surface plus outer glass with a low emissivity value and 6 mm thickness. The gap between the inner and outer glass is taken to be 13 mm. The physical characteristics of the building components and the window glass exposure rates are given in Table 1.

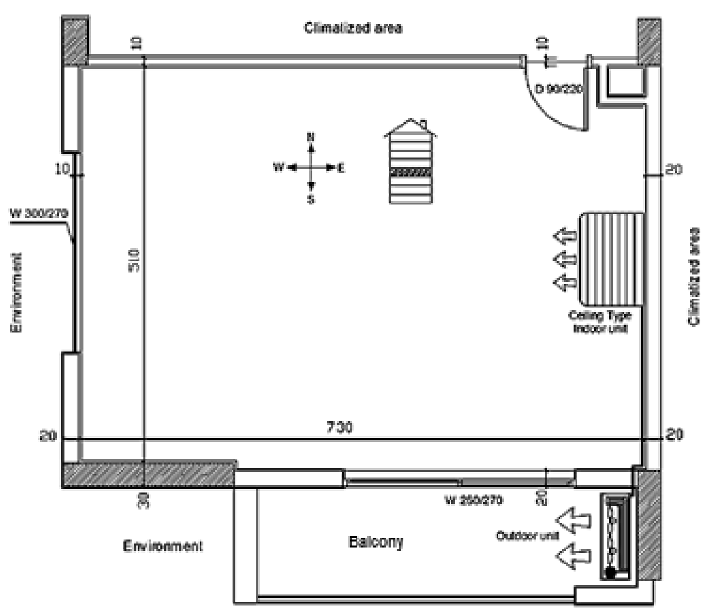

Fig. 2. Schematic view of a room in a building

The hourly cooling load capacities of the building for the months of April, May, June, July, August and September are determined using meteorological data, including solar radiation and atmospheric temperature (Liu & Jordan, 1960). The hourly total heat gain of the sample building is determined using the hourly analysis program (HAP) 4.8i by considering humans, illuminations, windows, walls and equipment (Bilgili, 2011). The hourly analysis program (HAP) is a computer tool and uses the ASHRAE-endorsed transfer function method for load calculations and detailed 8,760 hour-by-hour simulation techniques for the energy analysis. HAP estimates design cooling and heating loads for buildings in order to determine the sizes required for the HVAC system components. The cooling load calculations of the building are given in Table 2. Figure 3 illustrates the variation of the hourly cooling load for different months. As can be seen from this figure, the hourly cooling load capacities for different months achieves its maximum level at approximately 17:00 hours, because the building has an 8 m^2 window pane in a westerly direction. The maximum cooling load is calculated as 9.65 kW at 17:00 hours in August. The daily total load for that particular day is calculated as 185.85 kWh/day.

Table 1. Physical characteristics of the building components and window glass exposure

	Building components	**Thickness (cm)**	**Thermal conductivity (W/mK)**	**Density (kg/m^3)**	**Thermal resistance value (m^2 K/W)**
Outer wall	Inner plaster	2.0	0.700	1400	0.029
	Brick wall	20.0	0.5	1200	0.400
	Outer plaster	3.0	1.0	1800	0.030
	Rock wool	5.0	0.04	150	1.250
Inner wall	Staff	2.0	0.7	1400	0.029
	Brick wall	19.0	0.33	600	0.576
Floor	Parquet	0.6	0.20	800	0.030
	Smoothing layer	5.0	1.40	2000	0.036
	Reinforced concrete	20.0	2.50	2400	0.080
Glazing	**Transmissivity**	**Reflectivity**		**Absorptivity**	
Outer Glazing	0.501	0.315		0.184	
Inner Glazing	0.639	0.116		0.245	

Table 2. Total zone loads and envelope loads for Adana

ZONE LOADS		Details	Sensible (W)		Latent (W)	
Window & Skylight Solar loads		15 m²	3216		-	
Wall transmission		22 m²	873		-	
Roof transmission		0 m²	0		-	
Window transmission		15 m²	339		-	
Electric equipment		2500 W	2500		-	
People (Sensible and latent)		14	1005		841	
Safety factor		10%	793		84	
Total zone loads		-	8726		925	
ENVELOPE LOADS		Area (m²)	U-Value (W/m²K)	Shade Coeff.	Cooling Trans (W)	Cooling Solar (W)
South exposure	Wall	15	1.752	-	606	-
	Window	7	2.019	0.513	156	963
West exposure	Wall	7	1.752	-	267	-
	Window	8	2.019	0.513	183	2299

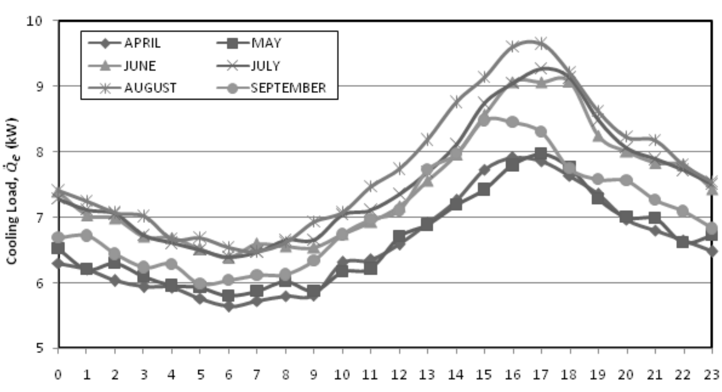

Fig. 3. Hourly variation of cooling load capacity of the building

Energy and exergy calculations

Technical specifications for components of the CTAC system are given in Table 3. Ten different refrigerants have been considered for the vapor compression refrigeration cycle. The system consists of four main parts, including compressor, condenser, capillary tubes and evaporator. Moreover, there is a 4-way reversing valve to use the system as a heat pump, and a check valve that allows refrigerant flow in any desired direction. A hermetically sealed and inverter-driven rotary compressor is used in the CTAC system. Minimum and maximum cooling capacities of the system vary between 2.6 kW and 12.0 kW, respectively. The system has two copper capillary tubes as an expansion device. Air volume flow rates of the outdoor and indoor units are 6060 m^3/h and 1650 m^3/h, respectively.

Table 3. Technical specifications for components of ceiling-type air conditioning system

Component	Technical specification
Cooling capacity (max.–min.)	2.6–12.0 kW
Nominal power	2.67 kW
Voltage	220/240, 1–50Hz
Air volume flow rate of outdoor unit	6060 m^3/h
Air volume flow rate of indoor unit	1650 m^3/h
Compressor Type	DC Twin Rotary

Exergy analysis results of the CTAC system for refrigerant R410A are given in Table 4 following the state numbers specified in Figure 1. The reference temperature (T_0) and reference pressure (P_0) for Adana province were determined to be 36.8 ^{o}C and 101.049 kPa, respectively. The thermodynamic properties of all refrigerants were determined using the CoolPack V2.85 software program. The effect of different refrigerants on the compressor power rates and COP values of the CTAC system are presented in Figure 4. It can be seen from this figure that the decrease in the actual work the compressor does (it is moved to the right side on the x-axis) improves the COP values of the CTAC system. The main reason for an increase in COP is the reduction of current drawn by the compressor. For example, when R404A refrigerant is used, the condenser outlet temperature (T_6) and heat rejected from the condenser are 42.73 ^{o}C and 11.89 kW, respectively. Furthermore, the actual power received by the compressor is 2.24 kW. When R600a refrigerant is used, the condenser outlet temperature, heat rejected from the condenser and the actual power received by the compressor are 42.59 ^{o}C, 11.59 kW and 1.94 kW, respectively. Changing the refrigerant from R404A to R600a reduces the air temperature at the condenser outlet from 42.73 ^{o}C to 42.59 ^{o}C. In conclusion, when R600a is used instead of R404A, the COP values of the CTAC system increase from 4.32 to 4.96.

Table 4. Exergy analysis results of the system for a sample refrigerant (R410A)

State No	Description	Fluid	Phase	Temperature (ºC)	Pressure (kPa)	Enthalpy (kj/kg)	Entropy (kj/kgK)	Mass flow rate (kg/s)	Specific Exergy (kj/kg)	Exergy Rate (kW)
				T	**P**	**h**	**s**	$\dot{m}$	**ψ**	$\dot{E}x$
0	-	Air	Dead state	36.8	101.049	-	-	-	0	0
0	-	Refrigerant (R410A)	Dead state	36.8	101.049	465.56	2.189	-	0	0
1	Evaporator outlet / Compressor inlet	Refrigerant	Superheated vapor	19.609	1069.1	437.373	1.839	0.05901	80.150	4.730
2	Compressor outlet / Condenser inlet	Refrigerant	Superheated vapor	81.313	3160.1	475.106	1.857	0.05901	112.400	6.633
3	Condenser outlet /Capillary tube inlet	Refrigerant	Liquid	81.313	3160.1	273.809	1.245	0.05901	100.700	5.942
4	Capillary tube outlet /Evaporator inlet	Refrigerant	Mixture	41.636	1069.1	273.809	1.261	0.05901	95.743	5.650
5	Condenser inlet	Air	Gas	36.8	101.049	-	-	1.993	0	0
6	Condenser outlet	Air	Gas	42.73	101.049	-	-	1.993	0.056	0.112
7	Evaporator inlet	Air	Gas	24.6	101.049	-	-	0.543	0.248	0.135
8	Evaporator outlet	Air	Gas	6.9	101.049	-	-	0.543	1.550	0.842

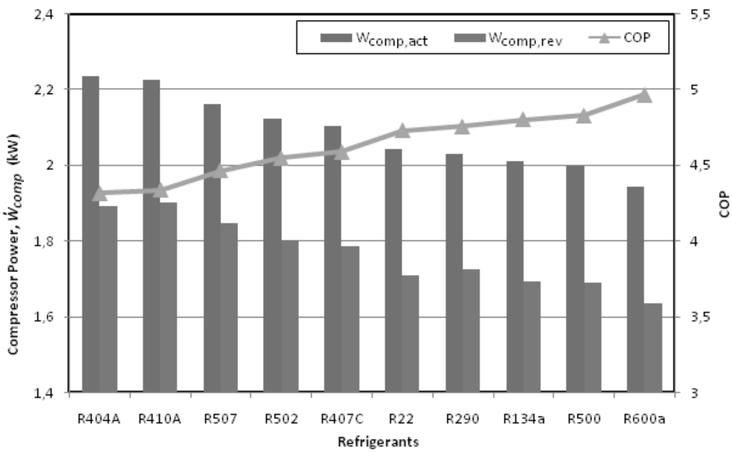

Fig. 4. Variation of refrigerants with compressor work and COP values

When R404A refrigerant is used in the CTAC system, the actual power received by the compressor motor is 2.24 kW. When the process is reversed, the compressor power is 1.89 kW for the production of the same useful work. When changing the refrigerant from R404A to R600a, the actual and reversible power values decrease to 1.94 kW and 1.64 kW, respectively. The results obtained from the present study are in a good agreement with the studies performed by Al-Joudi & Al-Amir (2014), and Kalaiselvam & Saravanan (2009).

The variation of exergy destruction of the CTAC system components by refrigerants is presented in Figure 5. As seen from the figure, the amount of exergy destruction decreases through the condenser, compressor and capillary tube, whereas the rate of exergy destruction does not change very much through the evaporator. When R404A refrigerant is used in the CTAC system, the maximum exergy destruction occurs in the condenser, amounting to 0.5 kW. Furthermore, the exergy destruction rates that occur in the evaporator, compressor and capillary tube are 0.211 kW, 0.345 kW and 0.360 kW, respectively. The minimum exergy destruction of 0.188 kW occurs in the capillary tube when R600a is used. The exergy destruction rates in the condenser, compressor and evaporator are 0.430 kW, 0.310 kW and 0.202 kW, respectively.

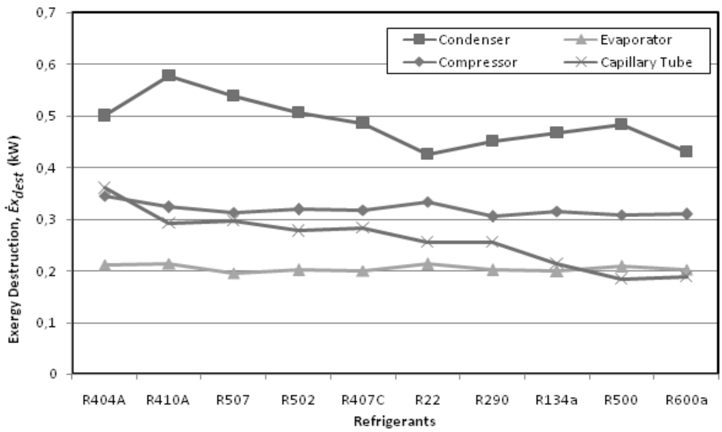

Fig. 5. Variation of exergy destruction of system components by refrigerant

Figure 6 illustrates the variation of exergy efficiency of the CTAC system components by refrigerant. Changing the refrigerant from R404A to R600a decreases the exergy efficiency for the compressor, evaporator and capillary tube. When R404A is used in the CTAC system, the maximum exergy efficiency obtained is 96.1 % in the evaporator. The other components of CTAC systems, such as capillary tube, compressor and condenser have exergy efficiencies of 93.6 %, 84.6 % and 18.3 %, respectively. On the other hand, when R600a is used, exergy efficiency values of the evaporator, capillary tube, compressor and condenser are 90.8 %, 91.6 %, 84.1 % and 19.9 %, respectively.

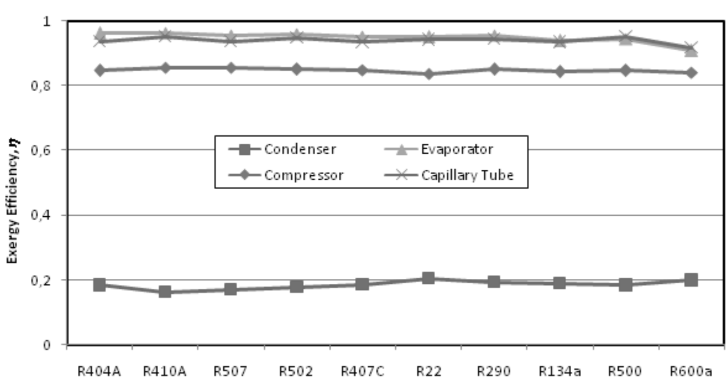

Fig. 6. Variation of exergy efficiency of system components by refrigerant

The variation of total exergy destruction and overall exergy efficiency by refrigerant is shown in Figure 7. As can be seen from this figure, the variation of total exergy destruction and overall exergy efficiency are inversely proportional to each other. It can be concluded that the total exergy destruction values in the CTAC system decrease when varying the refrigerant from R404A to R600a; however, overall exergy efficiency values of the system increase. While R404A is used in the CTAC system, the actual compressor power is calculated as 2.24 kW. In contrast, the total exergy destruction of the complete air conditioning system is found to be 1.417 kW. In addition, exergy destruction occurs in the evaporator with a value of 0.211 kW. Since there is no useful power in the evaporator, it should be equal to the reversible power. As a result, overall exergy efficiency of the refrigeration unit is determined to be 41.05 % when R404A refrigerant is used. When R600a is used, the actual compressor power supplied to the CTAC system is calculated to be 1.944 kW with a decrease of 13.0 %; the total exergy destruction value of the refrigeration system is found to be 1.13 kW with a decrease of 20.2 %; the exergy destruction of the evaporator is also determined to be 0.202 kW with a decrease of approximately 4.3 %; and the exergy efficiency of the refrigeration unit is finally found to be 46.7 %.

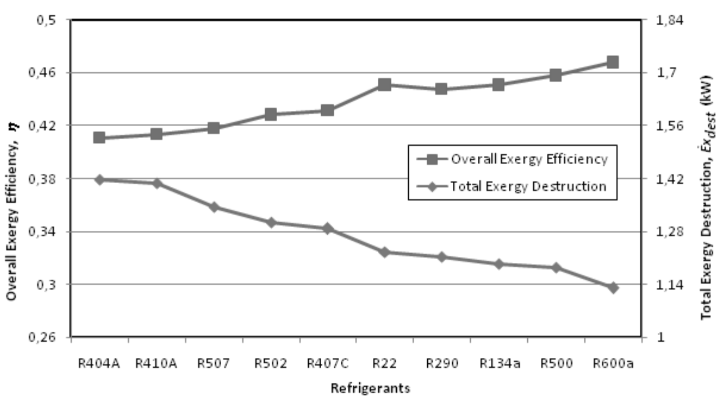

Fig. 7. Variation of total exergy destruction and overall exergy efficiency by refrigerant

CONCLUSIONS

This study investigates both energy and exergy analyses for the whole CTAC system, as well as its components, for different refrigerants. The various concluding remarks obtained from the results of this work can be summarized as follows:

- Changing the refrigerant from R404A to R600a increases the COP values of the overall refrigeration system from 4.32 to 4.96.
- When the refrigerant changes from R404A to R600a, the amount of exergy destruction decreases through the condenser, compressor and capillary tube, whereas the rate of exergy destruction does not change substantially through the evaporator.

- Overall exergy efficiency values of the system increase, when replacing the R404A refrigerant with R600a.
- Exergy destruction and exergy efficiency η, are inversely proportional to each other. That is to say, when R600a or R290 refrigerants are used instead of R404A, R410A or R502, the total exergy destruction values decrease. On the other hand, overall exergy efficiency values in the refrigeration system increase.
- R600a and R290 refrigerants, whose GWP values are lower, are a good alternative to R404A, R410A and R502 refrigerants, whose GWP values are higher in the CTAC system when considering the energy and exergy efficiency values.

ACKNOWLEDGEMENTS

The author would like to thank the office of Scientific Research Projects of Cukurova University for funding this project under Contract no. FBA-2015-3590.

REFERENCES

Al-Joudi, K.A. & Al-Amir, Q.R.A. 2014. Performance evaluation of small scale air-conditioning system using R22 and alternative refrigerants. Journal of Engineering, **1**(20):62-77.

Aprea, C., Greco A. & Maiorino, A. 2013. The substitution of R134a with R744: An exergetic analysis based on experimental data. International Journal of Refrigeration, 36:2148-2159.

Arora, A. & Kaushik, S.C. 2008. Theoretical analysis of a vapor compression refrigeration system with R502, R404A and R507A. International Journal of Refrigeration, 31:998–1005.

Bayrakci, H.C. & Ozgur, A.E. 2009. Energy and exergy analysis of vapor compression refrigeration system using pure hydrocarbon refrigerants. International Journal of Energy Research, 33:1070-1075.

Bilgili, M. 2011. Hourly simulation and performance of solar electric-vapor compression refrigeration system. Solar Energy, 85:2720–2731.

Bolaji, B.O. 2012. Performance of a R22 split-air-conditioner when retrofitted with ozone friendly refrigerants (R410A and R417A). Journal of Energy in Southern Africa, **23**(3)**:**16-22.

Cengel, Y.A. & Boles, M.A. 2004. Thermodynamics: an engineering approach, 5th ed., McGraw-Hill, NY.

Dincer, I. & Rosen, M.A. 2007. Exergy, Energy, Environment and Sustainable Development. Elsevier, Oxford, UK, 91-102.

Hurdogan, E., Buyukalaca, O., Hepbasli, A. & Yılmaz, T. 2011. Exergetic modeling and experimental performance assessment of a novel desiccant cooling system. Energy and Buildings, 43:1489–1498.

Kabul, A., Kizilkan, O. & Yakut, A.K. 2008. Performance and exergetic analysis of vapor compression refrigeration system with an internal heat exchanger using a hydrocarbon, isobutene (R600a). International Journal of Energy Research, 32:824–836.

Kalaiselvam, S. & Saravanan, R. 2009. Exergy analysis of scroll compressors working with R22, R407C, and R417a as refrigerant for HVAC system. Thermal Science, 13:175-184.

Liu, B.Y.H. & Jordan, R.C. 1960. The interrelationship and characteristics distribution of direct, diffuse and total solar radiation. Solar Energy, **4**(3):1-19.

Menlik, T., Ozcan, H. & Arcaklioğlu, E. 2014. Second law analysis of an environmentally friendly R290/R600/R600a mixture in a water-cooled heat pump unit. Journal of Thermal Science and Technology, **34**(2):19-28.

Padilla, M., Revellin, R. & Bonjour, J. 2010. Exergy analysis of R413A as replacement of R12 in a domestic refrigeration system. Energy Conversion and Management, 51:2195–2201.

Solmaz, O., Ozgoren. M. & Aksoy M.H. 2014. Hourly cooling load prediction of a vehicle in the southern region of Turkey by Artificial Neural Network. Energy Conversion and Management, 82:177–187.

Sun, X., Wu, J. & Wang, R. 2013. Exergy analysis and comparison of multi-functional heat pump and conventional heat pump systems. Energy Conversion and Management, 73:51–56.

Yan, G., Cui, C. & Yu, J. 2015. Energy and exergy analysis of zeotropic mixture R290/R600a vapor-compression refrigeration cycle with separation condensation. International Journal of Refrigeration, 53:155-162.

Submitted: 08/07/2015

Revised: 07/04/2016

Accepted: 14/04/2016